Indian Journal of Chemistry
Vol. 56A, January 2017, pp. 57-62

A comparative study of the photocatalytic properties of CuS nanotubes and nanoparticles by hydrothermal method

Xuyan You, Xiaohong Geng, Xiue Liu, Yang Yu & Zhihong Jing*

College of Chemistry and Chemical Engineering, Qufu Normal University, West Jingxuan Road No.57, Qufu, Shandong 273165, PR China
Email: zhhjing@126.com

Received 16 November 2016; re-revised and accepted 20 December 2016

Copper sulfide nanotubes and nanoparticles have been successfully synthesized by a hydrothermal process at 160 °C for 10 h, employing copper chloride ($CuCl_2 \cdot 2H_2O$) and thioacetamide as starting materials, polyethylene glycol 400 as surfactant. The products are characterized by X-ray power diffraction, scanning electron microscopy, UV–vis spectroscopy and fluorescence spectroscopy, respectively. The results show that both CuS nanotubes and nanoparticles belong to the hexagonal phase CuS and the morphologies of the products are greatly influenced by the surfactant, reactant molar concentration and reactant molar ratio. The photocatalytic properties of the CuS nanotubes and nanoparticles have been evaluated via photocatalytic degradation of organic dye and reduction of aqueous Cr (VI) under UV light irradiation. The CuS nanotubes with smooth inside and coarse outside present higher photocatalytic performance than the CuS nanoparticles.

Keywords: Photocatalytic degradation, Dye degradation, Hydrothermal synthesis, Surfactants, Nanotubes, Nanoparticles, Copper sulfide

Environmental pollution, broadly classified into three categories, viz., air, water and soil pollution, is a significant health risk and continues to threaten both human quality of life and the eco-system[1]. Among these, dye pollution poses a great threat to the environment due to its complicated structure, easy reaction with fiber, high adhesion ability, and resistance to biodegradation[2,3]. The common methods of treating organic wastes such as the biochemical and physical treatments have low degradation rate for treatment of the dye. Due to the better performance of semiconductor photocatalysts for the dye wastewater treatment by decomposing various organic pollutants at normal temperature, without secondary pollution, it is a new technology has an attractive application perspective in energy saving and environmental protection[4, 5]. In particular, transition metal sulfides, have wide applications because they are easily available and their shape and size can be controlled by changing reaction conditions like temperature, reactant concentration, surfactants and so on.

As an important p-type semiconductor, copper sulfide (CuS) exhibits many unusual electronic, optical, and other physical and chemical properties[6–9]. The use of CuS for degrading environmental pollutants has stimulated interest due to its high efficiency, nontoxic nature and low cost. In particular, nano-structured CuS has potential value on high photocatalytic activity because of their suitable bandgap and catalytic ability[10]. In the past few years, various attempts have been focused on the synthesis of CuS with different shapes, including nanoflakes[11], nanotubes[12], microspheres[13], nanoparticles[14], flower-like structures[15], nanowires[16], nanoribbons[17], nanorods[18], urchin-like structures[19]. Many methods of synthesis of copper sulfide nanotubes had been explored, such as template method[20], aqueous phase reaction[21], and hydrothermal process[22]. Various surfactants have been used in the hydrothermal synthesis, which play critical roles in the morphological control of CuS nanomaterial, like PEG-20000[23], CTAB[24] and SDBS[25].

In this study, CuS nanotubes and nanoparticles were prepared via a simple and one-pot hydrothermal process and their application in photocatalytic degradation of organic dye (rhodamine B and methyl orange) and reduction of aqueous Cr (VI) under UV light irradiation was investigated. The surfactant (PEG-400) and the reactant molar concentration ratio play an important role in determining the morphology, and then affect the photocatalytic activities of the CuS products.

Experimental

All the chemicals were of reagent grade and used without further purification. Copper chloride dihydrate ($CuCl_2 \cdot 2H_2O$), thioacetamide (TAA), potassium dichromate ($K_2Cr_2O_7$), polyethylene glycol-400 (PEG-400), rhodamine B (RhB) and methyl orange (MO) were purchased from Sinopharm Chemical Reagent Co., Ltd. (Shanghai, China).

CuS nanotubes were synthesized via a one-step hydrothermal method. Copper chloride (0.1705 g), thioacetamide (0.22553 g) and sodium hydroxide (0.004 g) were dissolved respectively in 30, 30 and 10 mL deionized water and labelled as solutions A, B, C, respectively. Firstly, solution B was added to solution A under constant stirring at room temperature for 10 min. Then, solution C and 4 mL PEG-400 were added slowly into the mixed solution. After that, the above mixture was transferred into a Teflon-scaled autoclave and maintained at 160 °C for 10 h. After completion of the reaction, the autoclave was air cooled to room temperature. The product was collected and washed three times with distilled water and alcohol, respectively, and dried at 80 °C for 24 h, denoted as S1.

Under the same conditions, instead of 4 mL PEG-400, 8 or 12 mL PEG-400 were used and the obtained products were denoted as S2, S3, respectively.

In absence of PEG-400, another series of experiments was carried out keeping the reactant millimol ratio ($CuCl_2 \cdot 2H_2O$/TAA/NaOH) as 1:3:1; 0.2:0.6:0.2 and 0.1:0.3:0.1, and the obtained products were denoted as S4, S5, S6, respectively.

The phase and the crystallinity of the samples were studied by X-ray power diffraction (XRD, Miniflex-600). The nanostructure and morphologies of samples were observed by scanning electron microscopy (SEM, JEOL JSM-6700F). The optical properties of samples were examined with fluorescence spectrophotometry (FL, F-7000) eV. The optical absorption was measured within the wavelength range 200–800 nm, using a UV–vis spectrophotometer (Agilent CARY-300, Austria).

The photocatalytic performance of the CuS samples was evaluated by the photogradation of RhB, MO and aqueous Cr(VI). $K_2Cr_2O_7$ was used as the sources of Cr(VI). The experiment was conducted in a homemade photocatalytic reaction apparatus. The CuS sample (60 mg) was added to 100 mL of the aqueous solution of RhB, MO and Cr(VI), respectively, which was magnetically stirring in the dark for 120 min to ensure an adsorption-desorption equilibrium. Then, the photoreaction vessel was exposed to UV irradiation (20 W mercury lamp) under magnetic stirring. At given time intervals, the photoreacted suspension (~3 mL) was analyzed by monitoring the absorption peak at 554, 464 and 260 nm (maximun absorption wavelength of RhB, MO and Cr(VI)) with a UV-vis spectrophotometer (752 Shanghai Jinghua Technology Instrument Co, China). The degradation efficiency of the photocatalyst can be defined as follows[26]:

$$\text{Degradation } (\%) = (1 - C/C_0) \times 100\%$$

where C_0 is the concentration of RhB, MO and Cr(VI) solution at the adsorption equilibrium and C is the residual concentration of RhB, MO and Cr(VI) solution at different illumination intervals. The photodegradation of RhB, MO and Cr(VI) solution follows pseudo-first-order kinetics, which can be expressed as follows:

$$\ln(C/C_\circ) = -kt$$

where k (min^{-1}) is the degradation rate constant.

Results and discussion

The XRD patterns of the six CuS products (S1-S6) are shown in Fig. 1. It was observed that the diffraction peaks matched well with the standard pattern of hexagonal CuS (JCPDS no. 06-0464). The peaks at 2θ = 27.554, 29.266, 31.621, 47.890, 52.599, 59.307 were indexed to the (101), (102), (103), (006), (110), (108), (116) planes of hexagonal CuS, respectively. No impurity peaks were observed, which indicated that high-purity crystalline CuS was successfully synthesized using this approach. The strong and sharp diffraction peaks in the XRD pattern indicate that the products were well crystallized. The average nanocrystallite size (D) of the samples S1, S2, S3, S4, S5, S6 was estimated using the Debye-Scherer formula ($D = 0.89\lambda/\beta\cos\theta$), to be 18.2, 19.3, 17.9, 21.9, 20.5, 19.3 nm.

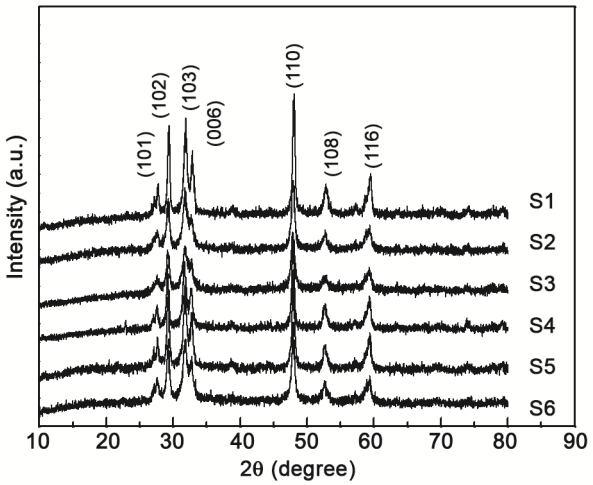

Fig. 1 – XRD pattern of the six CuS samples (S1-S6) obtained at 160 °C for 10 h by hydrothermal process.

The typical emission SEM images of the six CuS products are shown in Fig. 2(a-f). CuS nanotubes (S1) with an average diameter of 750 nm and length of 10 μm were observed. However, on increasing the amount of PEG-400 to 8 and 12 mL, CuS nanoparticles (S2 and S3) with an average diameter of 50-60 nm appear (see Fig. 2(b) and 2(c)). Interestingly, the CuS nanotubes (S1) exhibited smooth inside but coarse outside. Several nanoparticles, about 20 nm average diameters, aggregated and formed the coarse outside. This observation is in agreement with that of XRD.

To explore the influence of PEG-400 on the formation of CuS nanotubes, another series of experiments were carried out without PEG-400. The results were shown in Fig. 2(d-f). It can be see that in the absence of PEG-400, whether high or low concentrations of reactants, only nanoparticles (S4, S5 and S6) with an average diameter of 40–60 nm could be obtained, which suggests that the appropriate addition of PEG-400 is crucial for the formation of the CuS nanotubes. The effect of PEG-400 on the formation of CuS nanotubes may be explained as follows: (1) PEG-400 was a resolvable non-ionic surfactant and the PEG-400 monomer can easily form long chain structures in aqueous solution[27], which possibly served as a soft template, assisting in the formation CuS nanotubes; (2) With increased amount of PEG-400 as a dispersion medium, the aggregation of CuS crystals was reduced, hence the CuS showed homogeneous nanoparticle morphology with an average size of ~18 nm.

The morphologies of the CuS products (S1-S6) under different reactive conditions are given in Table 1. From Table 1, it can be seen that the surfactant and the amount of PEG-400 as well as the reactant molar concentration (or molar radio) give the CuS distinct morphologies.

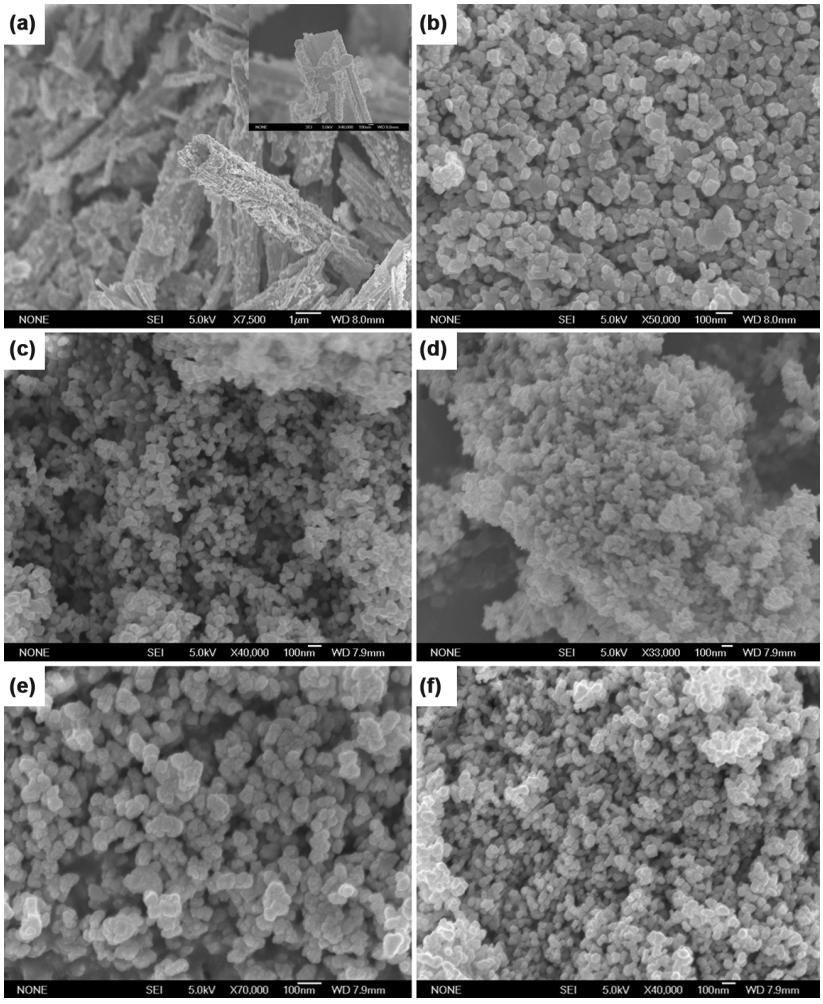

Fig. 2 – SEM images of the CuS nanotubes S1 (a) and the CuS nanoparticles S2–S6 (b-f).

In order to study the optical properties of the six CuS products (S1-S6), the room temperature fluorescence spectra were recorded and the results were shown in Fig. 3. Two strong emission bands centered at 403 nm and 471 nm for the CuS nanotubes (S1), and centered at 408 nm and 478 nm for the CuS nanoparticles (S2-S6), were observed when the excitation wavelength was 365 nm. The small blue shift of the S1 may be due to the structure of CuS nanotubes[28]. Our results are consistent with the PL results reported by Roy[28] and Ou[29]. According to these studies, the varying morphology of copper sulfide may be responsible for difference in photoluminescence phenomenon.

In addition, the UV-vis absorption of the CuS nanotubes (S1) and nanoparticles (S4) in the wavelength range 200–800 nm had been investigated (Fig. 4). A difference in absorbance of the CuS nanotubes (S1) and nanoparticles (S4) is observed; two absorption peaks were observed at 211 and 238 nm for CuS nanotubes (S1), while one absorption peak was observed at 269 nm for CuS nanoparticles (S4). Compared with bulk CuS (~344 nm), the as-prepared CuS nanotubes (S1) and nanoparticles (S4) exhibited a large and distinct blue-shift, which may be attributed to the special morphological effect of these products[29,30].

The photocatalytic activities of the four CuS products (S1-S4) were evaluated by the degradation of RhB and MO solutions under UV light irradiation. (The photocatalytic activities of the S5 and S6 were similar to that of S2-S4, omitted here). The degradation rates of the four CuS products (S1-S4) for RhB and MO at different intervals are shown in Fig. 5(a) and 5(b), respectively. About 87.3% of the RhB solution or 91.5% of the MO solution was degraded after 140 min for the CuS nanotubes (S1). The CuS nanotubes (S1) presented higher photocatalytic degradation efficiency as compared to the nanoparticles (S2-S4), Meanwhile, in order to examine the effect of products and UV light irradiation on the photodegradation, organic solutions in the absence of the CuS or UV light irradiation were tested under the same photocatalytic conditions; the results are shown in Fig. 5(a) and 5(b). In the absence of the CuS or UV irradiation, the concentration of organic solutions was almost constant during the irradiation, which illustrates that the CuS product and UV light irradiation were essential requirements for photocatalysis.

The kinetics of the degradation of RhB and MO solutions under UV irradiation was (Insets of Fig. 5(a) and 5(b)). We can see that all the CuS samples show linear plots, which indicate that the photodegradation follows first order kinetics. First order kinetics equations of the degradation of the four CuS products (S1-S4) for organic dyes are shown in Table 2. The

Table 1 – Morphologies of the six CuS products (S1-S6) under different experimental conditions

Sample	$CuCl_2 \cdot 2H_2O$ (mmol)	TAA (mmol)	NaOH (mmol)	PEG-400 (mL)	Morphology
S1	1	3	1	4	nanotubes
S2	1	3	1	8	nanoparticles
S3	1	3	1	12	nanoparticles
S4	1	3	1		nanoparticles
S5	0.2	0.6	0.2	0	nanoparticles
S6	0.1	0.3	0.1		nanoparticles

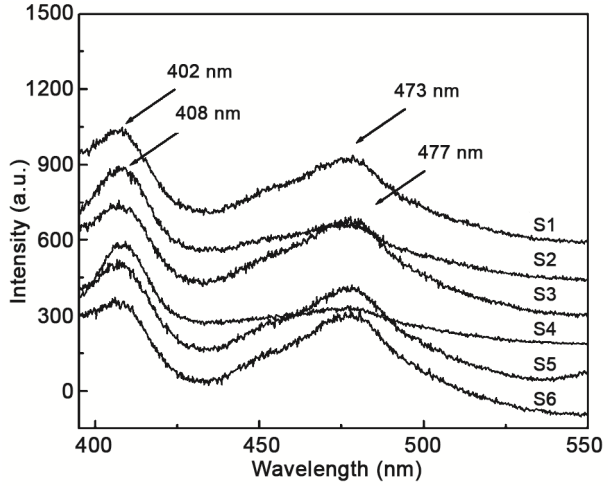

Fig. 3 – Fluorescence spectra of the six CuS samples (S1-S6) obtained at 160 °C for 10 h by hydrothermal process.

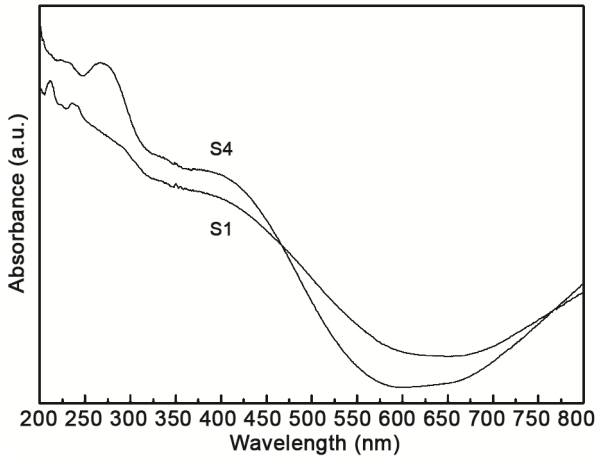

Fig. 4 – UV-vis absorption of the CuS nanotubes (S1) and nanoparticles (S4).

Table 2 – First-order kinetics equations of photocatalytic degradation of the four CuS products (S1-S4) for organic dyes

Sample \ Organic dye	Rhodamine-B	Methyl orange
S1	$\ln(C/C_0) = -0.05432 - 0.01462t$	$\ln(C/C_0) = -0.01765 - 0.01713t$
S2	$\ln(C/C_0) = -0.03883 - 0.00893t$	$\ln(C/C_0) = -0.03693 - 0.01241t$
S3	$\ln(C/C_0) = -0.13211 - 0.00981t$	$\ln(C/C_0) = -0.06435 - 0.01066t$
S4	$\ln(C/C_0) = -0.01459 - 0.00596t$	$\ln(C/C_0) = -0.03971 - 0.00681t$

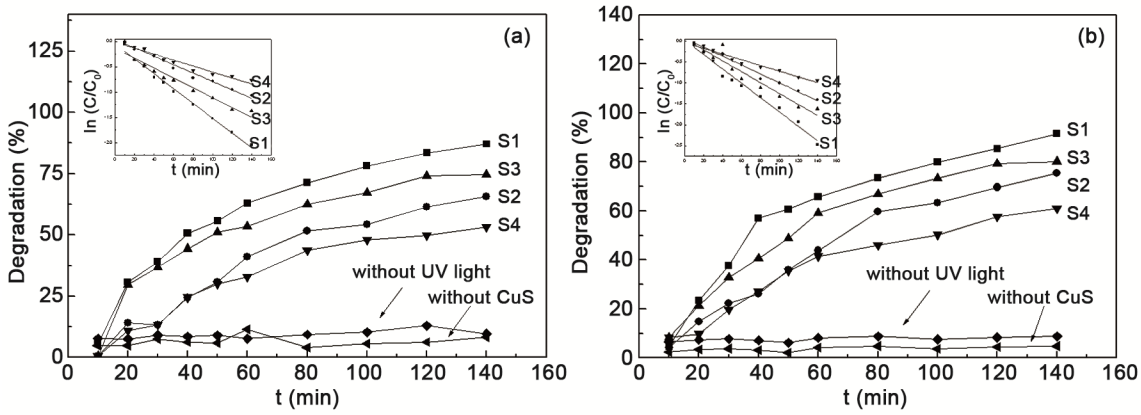

Fig. 5 – Degradation curves and first-order kinetics plots (Inset) of the degradation of CuS samples (S1-S4) for rhodamine B (a) and methyl orange (b).

apparent rate constants of RhB were determined as 0.01462, 0.00893, 0.00981 and 0.00596 min^{-1} for S1, S2, S3 and S4, respectively. The apparent rate constants of MO were determined as 0.01713, 0.01241, 0.01066 and 0.00681 min^{-1} for S1, S2, S3 and S4, respectively. Thus, the photocatalytic activity of the CuS nanotubes (S1) is much higher than that of the CuS nanoparticles in the present experiments. The reason may be due to the unique structure of CuS nanotubes. The CuS nanotubes with smooth inside but coarse outside consist of many nanoparticles; the nanoparticles located on the surface of the CuS nanotubes, produce a larger number of photocatalytic activity sites which may be responsible for the high photocatalytic degradation rate for the RhB and MO.

Cr(VI) is one of the most toxic pollutants found in the underground water sources and has been classified as carcinogenic and mutagenic[31, 32]. A common method of treating aqueous Cr(VI) is to convert it into Cr(III). Recently, the semiconductor photocatalytic reduction method has been widely used in treating aqueous Cr(VI)[33, 34]. Herein, we used the as-prepared CuS nanotubes (S1) and nanoparticles (S4) to investigate their application in photocatalytic reduction of aqueous Cr(VI) under UV light irradiation.

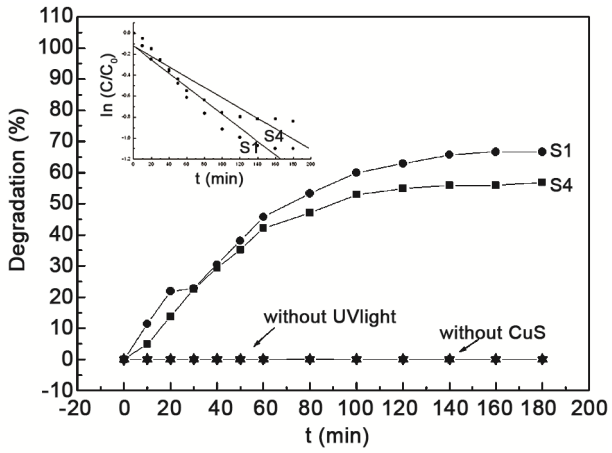

Fig. 6 – Degradation curves and first-order kinetics plots (Inset) of photocatalytic reduction of Cr(VI) of the as-prepared CuS nanotubes (S1) and CuS nanoparticles (S4).

Photocatalytic reduction of Cr(VI) in the absence of any photocatalyst or UV irradiation and in the presence of the as-prepared CuS nanotubes or CuS nanoparticles after exposure to UV irradiation are shown in Fig. 6, and the kinetics of the degradation

of Cr(VI) solutions under UV irradiation are shown in the insets of Fig. 6. In the absence of the CuS catalysts or without UV light irradiation, there is no obvious change in the Cr(VI) concentration. After irradiation for 140 min, nearly 65.7% of Cr(VI) was photocatalytically reduced by the CuS nanotubes (S1), while the removal rate of Cr(VI) by the CuS nanoparticles (S4) was only about 55.8% under the same conditions. The apparent rate constants of the Cr(VI) were determined as 0.00649 and 0.00492 min^{-1} for S1 and S4, respectively. Significantly enhanced photocatalytic activity can be seen with the CuS nanotubes (S1) in our experiments.

In summary, copper sulfide nanotubes or nanoparticles were successfully obtained by a simple one-pot hydrothermal synthesis. The obtained CuS nanotubes and five samples of CuS nanoparticles belong to hexagonal CuS. The CuS nanotubes demonstrate higher photocatalytic performance as compared to that of the CuS nanoparticles for degradation of RhB, MO and reduction of aqueous Cr(VI) under UV light irradiation. Considering the excellent photocatalytic behavior, the CuS nanotubes could be used in degradation applications for water purification.

Acknowledgement

This study was supported by the National Natural Science Foundation of China (Nos 21271115, 21501108).

References

1 Al-Ghouti M A, Khraisheh M A M, Allen S J & Ahmad M N, *J Environ Manag*, 69 (2003) 229.
2 Raffainer I I & Rohr R R, *Ind Eng Chem Res*, 40 (2001) 1083.
3 Bauer C, Jacques P & Kalt A, *J Photochem Photobiol A*, 140 (2001) 87.
4 Chen L, Zhang S, Wang L Q, Xue D & Yin S, *J Cryst Growth*, 311(2009) 735.
5 Zhang J, Yu J, Zhang Y, Li Q & Gong J, *Nano Lett*, 11(2001) 4774.
6 Córdova R, Gómez H, Schrebler R, Cury P, Orellana M, Grez P, Leinen D, Ramos-Barrado J R & Río R D, *Langmuir*, 18 (2002) 8647.
7 Lim W, Wong C, Ang S, Low H & Chin W S, *Chem Mater*, 18 (2006) 6170.
8 Erokhina S, Erokhin V, Nicolini C, Sbrana F, Ricci D & Zitti E D, *Langmuir*, 19 (2003) 766.
9 Gorai S, Ganguli D & Chaudhuri S, *Cryst Growth Des*, 5 (2005) 875.
10 Mills A, O'Rourke C & Moore K, *J Photochem Photobiol A: Chem*, 10 (2015) 66.
11 Zhang H, Wu G & Chen X, *Mater Chem Phys*, 98 (2006) 298.
12 Wang Q, Li J, Li G, Cao X, Wang K J & Chen J, *J Cryst Growth*, 299 (2007) 386.
13 Li B, Xie Y & Xue Y, *J Phys Chem C*, 111 (2007) 12181.
14 Dutta A & Dolui S K, *Mater Chem Phys*, 112 (2008) 448.
15 Thongtem T, Phuruangrat A & Thongtem S, *Curr Appl Phys*, 9 (2009) 195.
16 Wu C, Shi J, Chen C, Chen Y, Lin Y, Wu P & Wei S, *Mater Lett*, 62 (2008) 1074.
17 Tan C, Lu R, Xue P, Bao C & Zhao Y, *Mater Chem Phys*, 112 (2008) 500.
18 Roy P & Srivastava S K, *Mater Lett*, 61 (2007) 1693.
19 Zhu L, Xie Y, Zheng X, Liu X & Zhou G, *J Cryst Growth*, 260 (2004) 494.
20 Zhu Y, Guo X & Jin J, *J Mater Sci*, 42 (2007) 1042.
21 Nafees M, Ali S & Idrees S, *Appl Nanosci*, 3 (2013) 119.
22 Krishnamoorthy K, Veerasubraman G K, Rao A N & Sang J K, *Mater Res Exp*, 1(2014) 035006.
23 Ji H, Cao J, Feng J, Chang X, Ma X, Liu J & Zheng M, *Mater Lett*, 59 (2005) 3169.
24 Kundu J & Pradhan D, *New J Chem*, 37 (2013) 1470.
25 Wu C, Zhou G, Mao D, Zhang Z, Wu Y, Wang W, Luo L, Wang L, Yu Y, Hu J, Zhu Z, Zhang Y & Jie J, *J Mater Sci Technol*, 29 (2013) 1047.
26 Feng Y, Feng N, Zhang G & Du G, *Cryst Eng Comm*, 16 (2014) 214.
27 Liu Y, Hou Y & Wang G, *Mater Chem Phys*, 28 (2004) 69.
28 Roy P & Srivastava S K, *Cryst Growth Des*, 6 (2006) 1921.
29 Ou S M, Xie Q, Ma D K, Liang J B, Hu X K, Yu W C & Qian Y T, *Mater Chem Phys*, 94 (2005) 460.
30 Tanveer M, Cao C, Aslam I, Ali Z, Idrees F, Tahir M, Khan W S, Butt F K & Mahmood A, *RSC Adv*, 4 (2014) 63447.
31 Kleiman A, Marquez A, Vera M L, Meichtry J M & Litter M I, *Appl Catal: B*, 101 (2011) 676.
32 Yu H, Chen S, Quan X, Zhao H & Zhang Y, *Environ Sci Technol*, 42 (2008) 3791.
33 Zhang Y C, Li J, Zhang M & Dionysiou D D, *Environ Sci Technol*, 45 (2011) 9324.
34 Yang W, Liu Y, Hu Y, Zhou M & Qian H, *J Mater Chem,* 22 (2012) 13895.